Journal for Geometry and Graphics
Volume 28 (2024), No. 1, 103–116

3D Printing of Flat-Folded Bistable Origami-Like Structures

Pamela Higa[1], Yiyang Jia[2], Jun Mitani[1]

[1]*University of Tsukuba, Tsukuba, Japan*
a20061417@pucp.pe, mitani@cs.tsukuba.ac.jp

[2]*Seikei University, Musashino, Japan*
jiayiyang@st.seikei.ac.jp

Abstract. 3D printing has revolutionized manufacturing. However, its applicability has been limited due to lengthy printing times and the waste generated from the use of support materials. To address these limitations, this study introduces an approach for 3D printing of flat-folded structures. This approach utilizes bistable structures, which possess two stable states. We target structures consisting of connected bistable units. This alignment results in the formation of a tubular structure that follows a two-dimensional or three-dimensional curve. These structures have applications in product design, engineering, and architectural design. Additionally, the structures can be flat-folded and printed in this state, minimizing the use of support materials and printer space. We have demonstrated the functionality of this approach by printing models in a flat-folded state and then deploying them. To facilitate usage by designers, we have developed this system within the widely used Rhinoceros + Grasshopper environment.

Key Words: origami design, bistable structure, computer graphics, 3D printing
MSC 2020: 51-08

1 Introduction

3d printing or additive manufacturing technologies have seen a decrease in cost and increase in use for the past few decades. Additionally, the advances in accuracy and material availability led to widespread use in industry. Their printing time, support materials disposal and size constraints are the main limitations of additive manufacturing.

One approach to address such limitations is printing structures, in a folded state, and then unfolding them to the final product shape. Noma et al. [8] use curve origami and flexible hinges to reduce printing size, hence reducing material disposal and printing time. However, the range of shapes that can be printed using this method is limited, and the downsizing can be improved.

The goal of this research is to develop a system that enables the 3D printing of structures in a flat folded state without the need for assembly. Flat-foldable structures are shapes that can be folded until all their facets are parallel. Among the flat-foldable geometries, bistable structures [6], with two stable states will be the focus of our study. Structures capable of maintaining their volumetric shape without the application of external forces. These shapes were selected for their potential applications in fields such as robotics, architecture, and industrial design.

Melancon et al. [6] introduced a bistable inflatable arc, arranging two units with different deployment angles. While inspired by their work on bistable structures, our research focused on applying this approach to 3D printable objects. Additionally, we extend the range of shapes presented by arranging a series of units along a two-dimensional Bézier curve. Furthermore, we expand the design possibilities by introducing a method for adding a sloop, thereby accommodating the unit along a curve traced on a sphere.

Furthermore, various hinge techniques [1, 3–5] have been explored and applied to experimental printed models. Rigid origami geometric constraints were considered for the model design [9]. During the experiments, various materials and parameter values were tested until successful printing of the models in a flat folded state. A range of models was designed and printed, beginning with a basic hinged dihedral, then a four-degree vertex, and finally a bistable unit. During the process, minimum parameters such as thickness and gap between pieces were determined to ensure the deployability of the models.

1.1 Research Goal

In our research, the objective is to create a design and deployment system for the fabrication of bistable structures inspired by flat-foldable origami designs, which also uses 3D printing technology to produce the objects. The two-dimensional tubular structures designed by our system are flat-foldable, 3D-printable, and bistable. These structures have potential applications in fields such as product design, engineering, and architectural design. Our approach is mainly based on the bistable unit structure introduced in [6]. A unit is made of two basic two bottomless quadrilateral pyramid parts with an additional strip area between them (Figure 1a and 1b). For convenience, we call each bottomless quadrilateral pyramid in the unit a sub-unit.

In the construction process, previous studies [6] alternately use two types of units with different angles (the angle θ of each unit, refer to Figure 1a, along a two-dimensional arc. This approach results in an inflatable, bistable tubular structure. However, their technique allows only arc-shaped structures. In essence, their design represents an alignment over an underlying plane. Notably, this plane is orthogonal to every tangent vector of the flat-folding direction. Our goal is to increase the diversity of possible designs by enabling the arrangement of units along relatively arbitrary open curves (except for the curves with non-differentiable points) through the placing of isosceles triangles along a curve.

Furthermore, to overcome the limitation of their research (i.e., only permit arc-shaped structures), we propose a new type of unit to realize the alignment of bistable units along two-dimensional curves traced on a sphere. In this manner, we can also develop intrinsically 3D tubular structures with our design system. The corresponding 3D printable models will be printed in their flat-folded states.

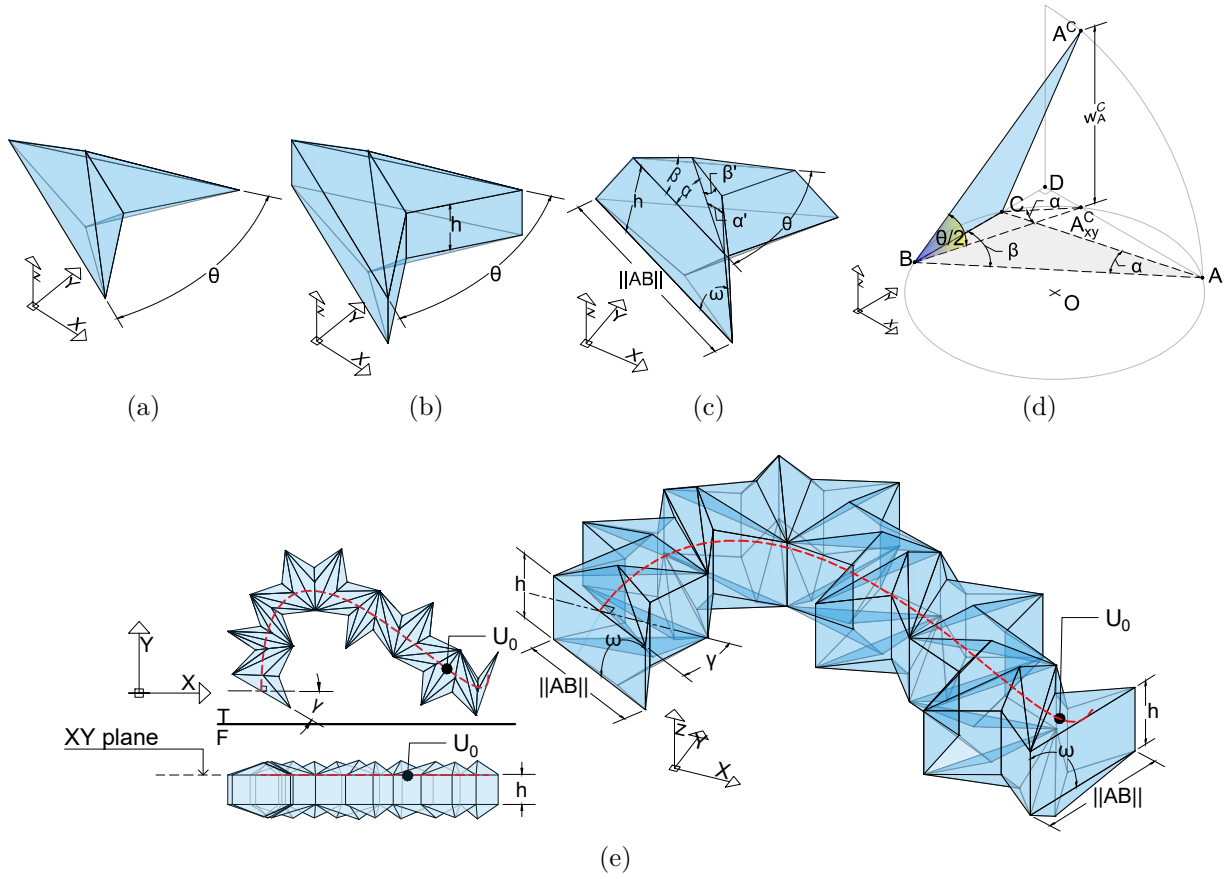

Figure 1: (a) The basic design of bistable units (two congruent sub-units are glued along their bottom edges). (b) A bistable unit with an intermediate rectangular connection component. (c) Design of bistable unit for the arrangement along a curve traced on a sphere. (d) Triangular building block. (e) Top, front and Isometric view of a sequence of bistable units arranged along a two-dimensional curve.

1.2 Proposed Method

At first, the basic principle of our design involves aligning a series of bistable units along a two-dimensional curve, to construct an intrinsically two-dimensional tubular structure. For this design, the corresponding design system requires the following inputs: a two-dimensional Bézier curve U_0; length of the line segment AB, denoted as $\|AB\|$; a ratio of $\|AB\|$ to h; and an angle γ which determines the orientation of the first unit (refer to Figure 1e).

The two-dimensional curve outlines the intended top-view shape that the structure will assume. The length $\|AB\|$ determines the size of the units, and the ratio $\|AB\|/h$ is used to calculate the height h of the intermediate strip between two sub-units. An initial input angle γ (refer to Figure 1e) specifies the angle between the first AB (of the first unit) on the XY plane and the tangent line at the endpoint of the input curve U_0, which in turn determines the specification of a sequence of angles $\{\theta_i\}$. The angles $\{\theta_i\}$ are the angles when the units reach deployed stable state. These terms will be introduced later. The additional input for the three-dimensional design, the angle ω, is depicted in Figure 1c. Roughly speaking, it adjusts the slope with which the units align along the curve traced on a sphere. A more comprehensive explanation of the inputs will be provided in Sections 3.2 and 4. Finally, our system will generate bistable, flat-foldable designs that are suitable for 3D printing. These

designs will be along either a two-dimensional or a curve traced on a sphere, all of which maintain a tubular shape.

2 Previous Strategy

In this section, we introduce the geometrical properties of the basic units proposed in [6] and how they were assembled. Especially, we will focus on the constraints arising from bistability. Finally, we will analyze the limitations and shortcomings of these components.

The purpose of [6] is to present a collection of origami-based structures for building substantial inflatable systems. These constructions fall under the self-folding origami design category with an external force generated by inflation, which further satisfies self-lockability and bistability. The fundamental sub-unit of their structure is a bottomless quadrilateral pyramid, as illustrated in Figure 1a, made of two pairs of compatible symmetric triangular building blocks. The triangular building blocks are defined by the points A, B and C. The point A will rotate around the AC axis, as shown in Figure 1d. It is observed that during the rotation, the projection of vertex A must move along the line segment AD.

A particular state exists in which the projection of A aligns with the circle circumscribed by vertices A, B, and C. In this state, the projection of A^c on the XY plane forms an angle $\alpha_{xy} = \alpha$. The displacement w_A^C is defined in [6] as follows.

$$w_A^C = \sqrt{1 - \frac{\cos^2(\beta_i)}{\sin^2(\alpha_i + \beta_i)}}. \tag{1}$$

This point corresponds to a stable state, distinct from the flat-folded state. Any state intermediate between the flat-folded state and this stable state is unstable due to geometric frustration. To achieve continuous deformation between these two stable states, in [6], they linked stiff triangular faces with stretchable hinges.

They further calculated the relationship between angles α and β, operating under the premise that $\alpha_{xy} = \alpha$ can only occur when both $\angle ACB$ and the central angle $\angle AOC$ are obtuse. The constraint is expressed in the following formula:

$$\alpha \in \left[0, \tfrac{\pi}{2}\right], \quad \beta \in \left[\tfrac{\pi}{4} - \alpha, \tfrac{\pi}{2} - \alpha\right].$$

They qualified and investigated the volume of each quadrilateral pyramid, defined by vertices on A^C, A_{xy}^C, B, and C. They also explored the incompatibility (or instability) brought about by geometric frustration, as well as the inflation and deployable constraints. Finally, they concluded that closed origami-based designs(which means the base curve is closed) cannot be realized by this system because it is impossible to satisfy both bistability and inflatability simultaneously. Given that our design system is based on a similar shape of units, it is unable to realize closed origami-based designs, either.

They subsequently shifted their focus to open origami-based designs and succeeded in establishing a system for creating designs along arcs. In our research, we expand their design approach, enabling designs not only along two-dimensional arcs but also along two-dimensional curves of relatively arbitrary shapes (provided they remain open and without any non-differentiable points) and along a curve traced on a sphere.

3 Bistable Units Along a Two-dimensional Curve

In [6], the authors presented a design method that alternately aligns two types of units with different angles α and β along an arc. In our research, we aim to increase the diversity of possible shapes by extending the shape of the base two-dimensional curve to arbitrary shapes as long as it remains open and without any non-differentiable point, otherwise. The presence of such factors would result in over-lapping units. To achieve this, we first place isosceles triangles along the curve and then define the unit in terms of the result of the placement.

3.1 Place Isosceles Triangles Along the Curve

The shape of the entire structure is primarily determined by the input two-dimensional curve, which can have a relatively arbitrary shape, unlike the arcs used in [6].

Our method begins by placing isosceles triangles along the curve on the same plane, designated as the XY plane in our system. The parameters for such a triangle include the length of the two legs, $\|AB\|$, apex angle θ, and direction of initial AB, determined by the angle γ. The length $\|AB\|$ is included in the input and constant along all the triangles, while the apex angle θ can vary among different triangles along the curve. We denote the set of these angles as $\{\theta_k \mid k \in \mathbb{N}\}$ and compute them sequentially based on the inputs. After the triangle placement, we arrange the units (which will be introduced in the next section) according to $\{\theta_k\}$ along the input open two-dimensional curve.

The input Bézier curve is supposed to be generated from n control points P, being $\{n > 1 \mid n \in \mathbb{N}\}$. The input curve is required to be an open curve, as opposed to a closed one, to prevent the possibility of unit overlap. Therefore, we utilize these control points to accomplish the placement of the triangles using the following steps (see Figure 2c and 2d).

1. Connect the first (P_0) and second control points (P_1) with a line segment, denoted as l.
2. Draw a line segment, AB_0, with length $\|AB\|$, perpendicular to l. The midpoint of AB_0 should coincide with P_0.
3. Rotate AB_0 around the first control point of the curve, by an angle of γ.
4. Draw an circle with a radius of $\|AB\|/2$, centered at B_0, B_0 is considered as the endpoint of AB_0 on the concave side of the curve. Record the intersection of the arc with the curve as the midpoint of the new line segment AB_1 and B_0 as the initial point of the new line segment AB_1.
5. Repeat Step 4 to create new line segments AB_k until no new intersection between the circles and the curve is found.

The internal angles between AB_i and AB_{i+1} are the angles θ_i. The above process determines the precise projection of each unit onto the XY plane. This, in turn, establishes the extent to which each unit is deployed. We translate the outcome of this process into $\{\theta_k\}$. The range of each θ_k will be detailed in Section 3.2.

3.2 Adjusted Design of the Unit

We use one of the bistable units proposed in [6], with the strip section located between two bottomless quadrilateral pyramids (as depicted in Figure 2a). A bottomless quadrilateral pyramid comprises two pairs of equilateral triangles, as seen in the blue and green areas in Figure 2b. These are referred to as ABC and $A'B'C'$, respectively. The angle, θ, must be considered when two equilateral quadrilateral pyramids are joined together to reach a deployed state. Moreover, for the triangles ABC and $A'B'C'$ to simultaneously achieve their

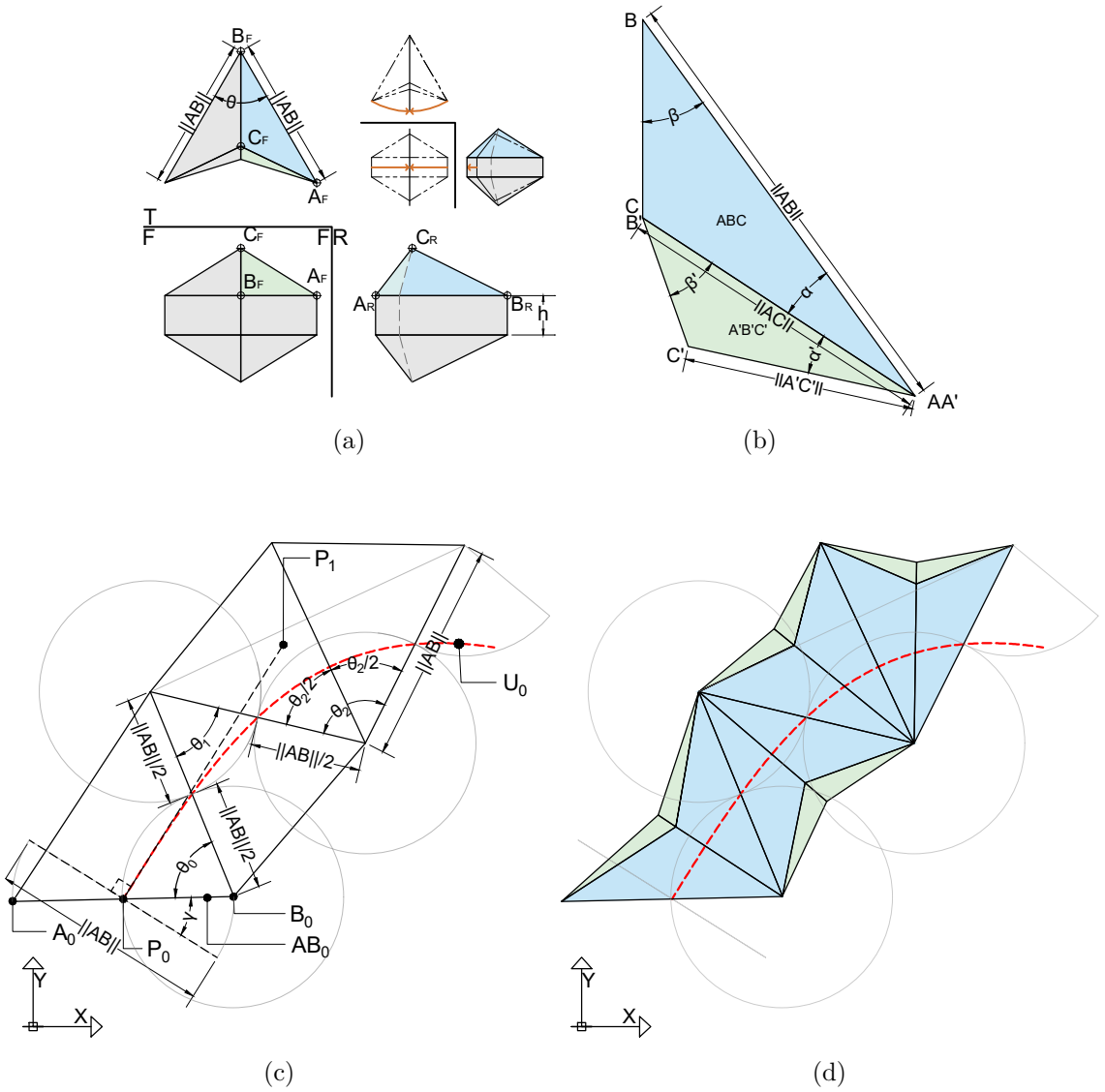

Figure 2: (a) Top, front, and side view of a bistable unit. The movement of the unit is illustrated in the upper-right corner. (b) Top view of two types of triangular which comprise the unit. (c) The placement of isosceles triangles along an input two-dimensional curve with parameter inputs $\|AB\|$ and γ. (d) How the bistable units are arranged along the input two-dimensional curve.

stable states, their respective α values must be equal, i.e., $\alpha = \alpha'$, which also gives rise to the following formula [6]:

$$\beta' = \arctan\left(\frac{\sin\beta}{\cos(\beta+\alpha)\cos\alpha} - \tan\alpha\right). \tag{2}$$

The unit to utilize is supposed to be defined in terms of the angles α and β of the triangle building block, and the length of every AB, $\|AB\|$. Correspondingly, the output of this triangle placement process includes the specialized line segments $\{AB_i\}_{i\in\mathbb{N}}$ fixed on the plane and the angles $\{\theta_i\}_{i\in\mathbb{N}}$. The following equation defines each θ_i in relation to the pair of angles

(α_i, β_i), refer to Figure 1(e):

$$\frac{\theta_i}{2} = \arcsin\sqrt{1 - \frac{\cos^2(\beta_i)}{\sin^2(\alpha_i + \beta_i)}}. \tag{3}$$

Since in the showed formula (3), θ_i is totally decided by (α_i, β_i),every combination within the range of α_i and β_i, yields a corresponding θ_i. When we further extend the result, to arrange the bi-stable units on a curve traced on a sphere (which will be introduced in the next section), these angles and the relationship between them will be redefined. In the next section, we show that for each θ_i, there is only one corresponding setting of (α_i, β_i) that satisfies the geometric constraints for the unit for the curve traced on a sphere. For convenience, we denote them without the subscript in the next section.

4 Adding Slope to the Array of the Bistable Units

In this section, we first investigate the geometry of the shape formed by three connected units (see Figure 3a). Its projection onto the XZ plane emulates the shape of an arc. Following this, we will further discuss the geometric constraints of our design for a curve traced on a sphere. The design is then implemented as a program running in the Rhinoceros + Grasshopper environment.

Our design employs units made up of two differently-sized quadrilateral pyramids. A bistable state requires that each unit must consist of the same pair of different bottomless quadrilateral pyramids. These two kinds of quadrilateral pyramids are distinguished by their sizes; the larger one is called the outer sub-unit, and the other is called the inner sub-unit (see Figure 3b).

The area between two quadrilateral pyramids in each unit is designed as a group of trapezoids, the trapezoids that represent the contact area between units are denoted as contact trapezoids, and the trapezoids bordering the structures are denoted as border trapezoids. Note that when designing bistable units along a two-dimensional curve, the shape degenerates into a rectangle. Since all the units share the same $\|AB\|$, the trapezoids should share the same shape. We denote the length of the longer base of the contact trapezoids as $\|AB\|_{\text{out}}$(i.e., the length of the base of the outer sub-unit), the length of the shorter base $\|AB\|_{\text{in}}$ (i.e., the length of the base of the inner sub-unit), and the height h.

We must employ isosceles trapezoids to connect the units due to their symmetrical nature. The acute base angle is defined as an input, denoted by ω. As illustrated in Figure 3d, the endpoints of AB_{out} and AB_{in} are positioned on two distinct spheres, both of which share the same center point. As a result, this design is only applicable to curves traced on a sphere (see 3c).

The reason is that each group of trapezoids, representing each unit, should be embedded on the surface of a quadrilateral-based pyramid with a vertex labeled as V. If another group of trapezoids is placed adjacent to it, sharing a contact trapezoid, they would also share the vertex V (see Figure 3c). This would result in all endpoints of the longer base of the contact trapezoids aligning on the same sphere and all endpoints of the shorter base aligning on a smaller sphere.

The four trapezoids form a shape as illustrated in Figure 3d. Due to the requirement for flat-foldability, the extensions of their legs should converge at the same vertex V. This vertex is determined by the angle ω. Following the constraints of flat-foldability of Kawasaki

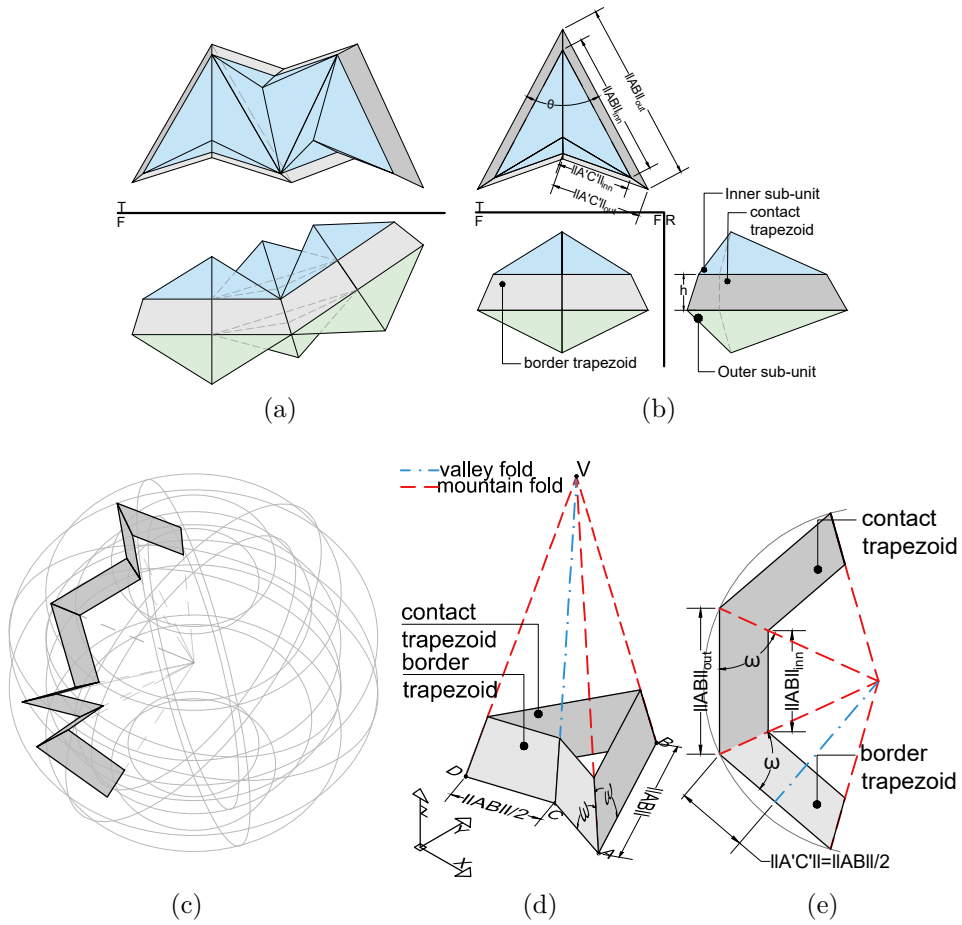

Figure 3: (a) Three connecting bistable units along a curve traced on a sphere. (b) A single bistable unit for a curve traced on a sphere, whose inner sub-unit is colored blue, the outer sub-unit is colored green, and the intermediate strip made of trapezoids is colored grey. (c) A sequence of connecting isometric isosceles trapezoids with their endpoints located on two concentric spheres. (d) Intermediate area between two bottomless quadrilateral pyramids. (e) Unfolded intermediate area.

theorem [2], a vertex can be considered flat-folded when the alternating sum and difference of the angles at that specific vertex equals zero. The base lengths of the two smaller trapezoids in Figure 3d should be $\|AB\|/2$, whereas the two larger trapezoids should have base lengths of $\|AB\|$. That is, $\|A'C'\| = \|AB\|/2$ (see Figure 3d, 3e). Consequently, we can derive the following formula, where α' and β' are depicted in Figure 2b:

$$\frac{\|AC\|\sin(\beta)}{\cos(\frac{\pi}{2} - (\alpha' + \beta'))} = \frac{\|A'C'\|}{\|AB\|} = \frac{1}{2}. \tag{4}$$

As aforementioned, $\alpha' = \alpha$ and the relationship between β' and β follows Equation (2). We compute the ratio $\|A'C'\|/\|AB\|$ and visually represent it using Grasshopper and AutoCAD, as depicted in Figure 4a, where the Z component representing the result of the $\|A'C'\|/\|AB\|$ equation, the Y component representing β, and the X component representing α. The grid-like blue surface represents all possible combinations of the triplet (α, β, $\|A'C'\|/\|AB\|$). The red two-dimensional curve represents the solution set where $\|A'C'\|/\|AB\| = \frac{1}{2}$.

The combinations of α and β that yield $\|A'C'\|/\|AB\| = 1/2$ can be determined by

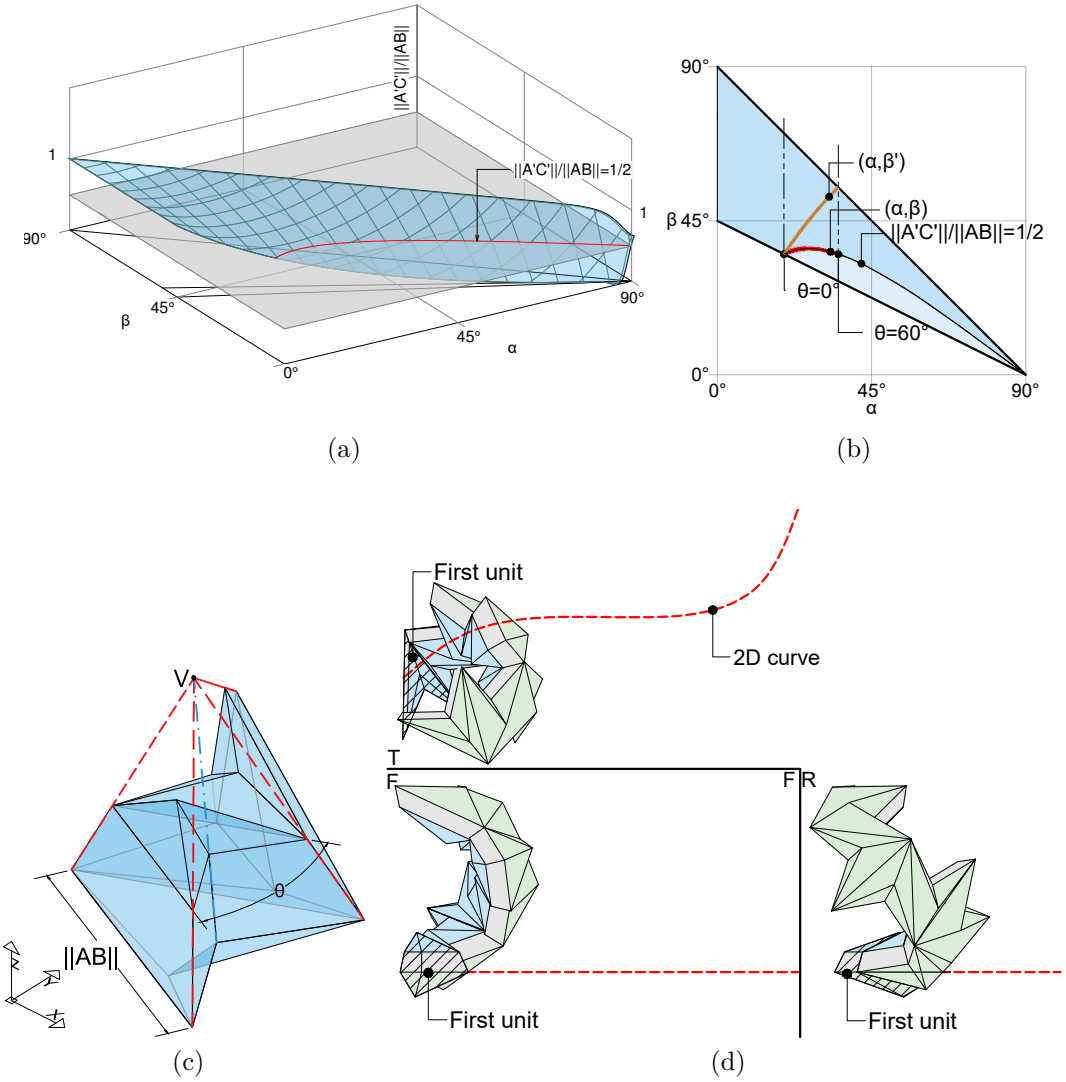

Figure 4: (a) A three-dimensional vision illustrating the ratio of the $\|A'C\|/\|AB\|$ in terms of α and β. The red curve indicates the solution set of (α, β). (b) The top view of illustration (a), which indicates the range of θ. The orange curve indicates the solution set of (α', β'). (c)Two units for a curve traced on a sphere. (d) Top, front, and side view of an arrangement of the bistable units along a curve traced on a sphere.

examining the projection of the solution curve, as depicted in Figure 4a. In Figure 4b, the corresponding combinations of α' and β' for each α and β combination are represented by an orange line. It is evident from the figure that the range of θ is constrained by the resulting values of α' and β'. Linking this finding with Equation (3), we conclude that $0 < \theta < \frac{\pi}{3}$.

The input angle ω will define the location of the center vertex V as shown in Figure 4c, V also is the center point of the sphere where the inputted two-dimensional curve is traced (refer to 3d).

5 3D Printing

Our objective includes devising a more efficient process for producing bistable structures using 3D printing. In this aspect, our design is highly compatible with this objective, as it allows

for the structures to be printed in a flat-folded state. We successfully 3D printed various hinged designs, starting with a basic hinged dihedral to a bistable unit.

To identify the most suitable technique, we first separately tested the hinged dihedral, i.e., the hinge between every pair of neighboring faces. Some of the practically tested components are shown in Figure 5b and 5c, which have different parameters. Next, we tested the combination of four faces together, we refer to the entire of these four hinges as a Hinged four-degree vertex [12] (see Figure 5e–5i). The final experiment consisted of printing a bistable unit for a three-dimensional curve (Figure 6c and 6d). Throughout the manufacturing process, all components were printed in their flat-folded states.

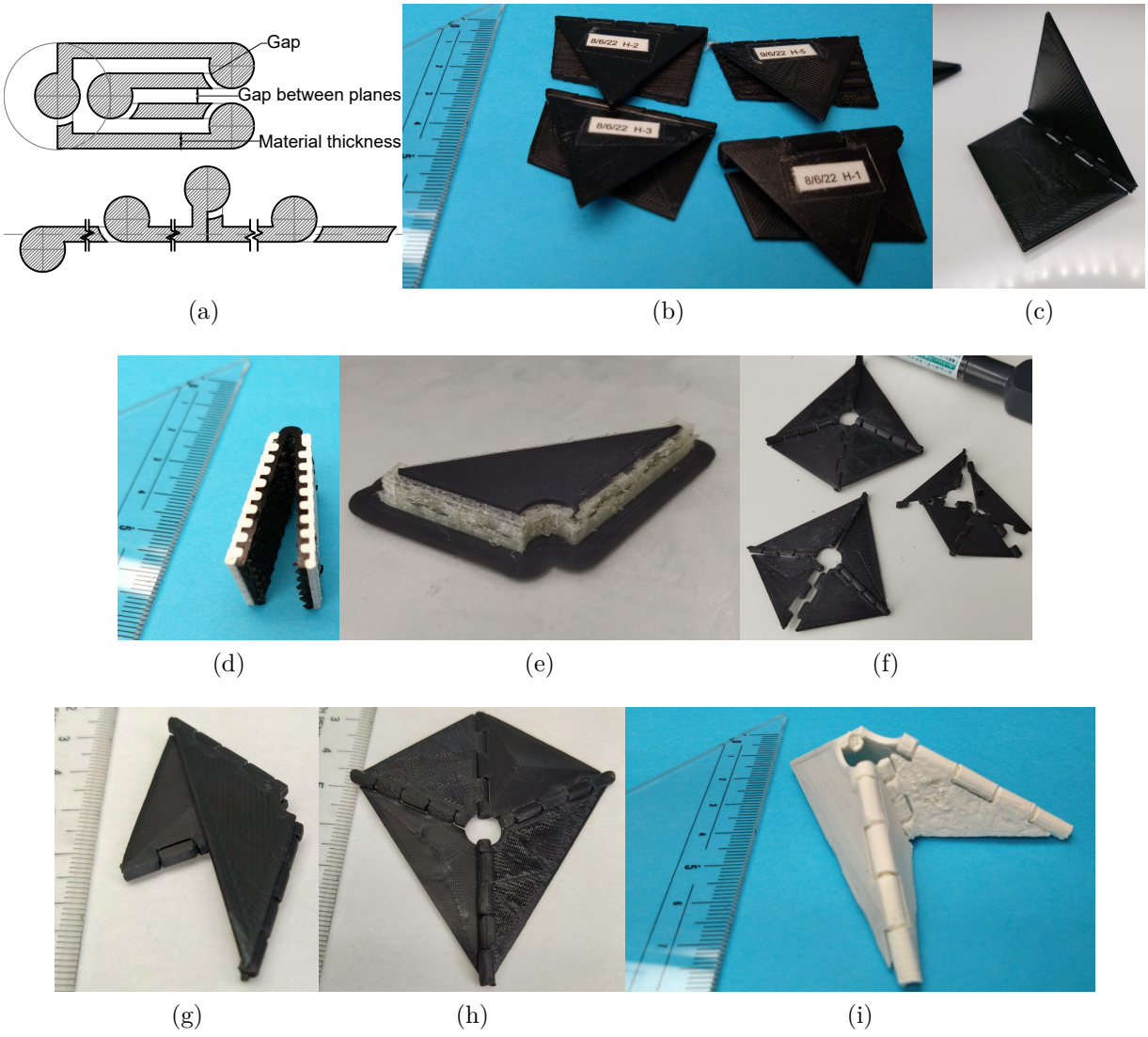

Figure 5: 3D printing results. (a) Hinge design, side view of its flat-folded state and its unfolded state. (b) Examples of our printed dihedral rotational hinges (Hinges 1,2,3 and 5). (c) Example of functional dihedral rotational Hinge (Hinge 4). (d) An example of our printed dihedral flexible hinges (Hinge 6). (e) An example of a developable four-degree vertex with rotational hinges and support material. (f) Photo of Hinges 7, 8, and 9. Hinges 7 and 8 failed and broke during deployment, while Hinge 9 successfully deployed. (g) An example of a developable four-degree vertex (Hinge9). (h)The unfolded state of the printed four-degree vertex (Hinge9). (i) An example of a non-developable four-degree vertex.

5.1 Hinged Dihedral

Two materials were evaluated for a hinged dihedral: rigid PLA and flexible TPUa. For the PLA hinge, the "Axis Shift Technique" [10] was used with PVA (water soluble) support material. Segmented hinges enabled rotation, with results for different segmentation shown in Table 1 and Figures 5b and 5c. Specifically, the materials were 0.4 mm black PLA for the main structure and 0.4 mm natural PVA for support. Figure 5d shows a TPUa hinge attached to a rigid PLA face without segmentation. Bonding the printed PLA and TPUa materials presented a key challenge due to their differing physical properties [11]. To address this, an interlaced chess pattern between materials was implemented[7].

Comparing the results, we found that the rotational hinge made of PLA outperformed the flexible hinge. The rotational hinge technique allows for printing with support materials, enabling the creation of complex shapes, which aligns well with our design requirements. Conversely, the flexible hinge requires two extruders for printing, one for PLA and one for TPUa. This limitation also precludes the use of soluble support materials. Therefore, the rotational hinge made of PLA was chosen for further experimentation.

Table 1: Hinged dihedral- rotational hinge

Hinge Parameters	**Hinge1**	**Hinge2**	**Hinge3**	**Hinge4**	**Hinge5**	**Recommended Values**
Rotation Angle (degrees)	0	8	0	0	5	0º
Num of Segmentations	3	5	5	7	7	>5
Gap length (mm)	1	0.6	0.2	0.4	0.4	0.4
Gap between planes (mm)	3	0	1.2	0.8	0	0.8
Face thickness (mm)	1.5	1	0.8	0.8	0.6	0.8
Print time (min)	45	53	29	22	25	
Profile (mm)	0.3	0.2	0.3	0.3	0.3	
length x (mm)	45	45	45	45	45	
length y (mm)	36	36	36	36	36	
length z (mm)	6	7	03	2.4	4	

The failed ones are colored red, and the optimal ones are colored green.

5.2 Hinged Four-Degree Vertex

Next, we assessed the performance of a Hinged four-degree vertex with the aforementioned rotational hinges made of PLA. Since we need to print the unit with all four hinges together, we print it in its flat-folded state. Considering the overall thickness and overlapping, we represent the flat-folded state by its side view, as illustrated in Figure 5a. To enhance robustness, we thicken the face. Three models were printed under these conditions, as depicted in Figure 5f, 5g and 5h, and the experimental results are provided in Table 2.

Additionally, we printed a non-developable four-degree vertex, varying the parameters in the same manner. The printed model is depicted in Figure 5i.

5.3 Bistable Unit

Next, a model for a flat-folded bistable for a three-dimensional curve unit was designed for printing. Achieving the desired bistability involves careful consideration of hinge alignment.

Table 2: Hinge Group for a four-degree vertex

Hinge Parameters	**Hinge7**	**Hinge8**	**Hinge9**	**Recommended Values**
Rotation Angle (degrees)	0	0	0	0
Num of Segmentations	5	5	5	5
Gap between planes (mm)	0.4	0.8	0.6	0.6
Face thickness (mm)	0.8	0.8	1.2	1.2
Print time (min)	23	43	93	
length x (mm)	30	20	50	
length y (mm)	25	36	32	
length z (mm)	4	5.6	6.6	

The values that lead to failure are represented in red, while the minimum successfully values are highlighted in green.

The incorporation of a double hinge, referred to as 'Offset crease' in [3], was necessary to achieve the desired movement, as illustrated in Figures 6a and 6b. This design comprises two parallel hinges with a small gap between them, facilitating free rotation of the panels without interference. Due to its intricate shape, the model was printed with high-resolution acrylic and successfully deployed with 1 degree of freedom (1DOF) movements, as intended (see Figure 6c and 6d).

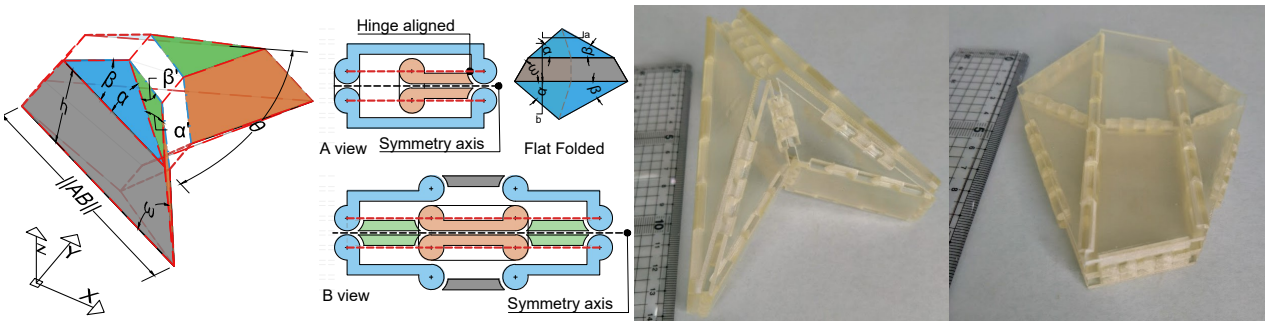

(a) (b) (c) (d)

Figure 6: Bistable Unit for 3D Printing. (a) Isometric view of the geometry of a bistable unit with a double hinge. (b) Sides views of the hinged bistable unit. (c) Printed model of a bistable unit, deployed. (d)Printed model of a bistable unit, flat-folded.

6 Conclusion and Future Work

In this research, we investigated 3D printable bistable structures based on origami designs. We renovated the design from [6], and proposed a method for constructing curved designs applicable to both two-dimensional and curves traced on a sphere. The unit can be relatively freely decided by users through the user interface (parameters) of our system. We have also experimented with our design using the 3D-printing technique in practice. The origami-based design enables easy printing of components from a flat-folded state, demonstrating the potential for industrial manufacturing of these structures. This approach is particularly useful for the design of space-saving items that expand into functional shapes when needed.

So far, our design system is limited to creating shapes that follow a specific type of curve, namely, those located on a sphere. This limitation arises from the triangle placement method. Moreover, due to this same reason, our system is incapable of handling any form of closed curve input. In future work, our objective is to 3D-print the entire bistable structure along a curve traced on a sphere. This will entail connecting the units with rotational double hinges, employing methodologies reminiscent of those previously used. Subsequently, our focus will shift towards extending the adaptability of this system to accommodate a variety of curve types beyond the current ones supported.

Acknowledgement

This work was supported by JST CREST Grant Number JPMJCR1911, Japan.

References

[1] J. A. Faber, A. F. Arrieta, and A. R. Studart: *Bioinspired spring origami*. Science **359**(6382), 1386–1391, 2018. doi: 10.1126/science.aap7753.

[2] T. Kawasaki: *On the relation between mountain-creases and valley-creases of a flat origami*. In *Proceedings of the First International Meeting of Origami Science and Technology, 1991*. 1991.

[3] J. S. Ku and E. D. Demaine: *Folding flat crease patterns with thick materials*. Journal of Mechanisms and Robotics **8**(3), 031003, 2016. doi: 10.1115/1.4031954.

[4] R. J. Lang, N. Brown, B. Ignaut, S. Magleby, and L. Howell: *Rigidly foldable thick origami using designed-offset linkages*. Journal of Mechanisms and Robotics **12**(2), 021106, 2020. doi: 10.1115/1.4045940.

[5] R. J. Lang, K. A. Tolman, E. B. Crampton, S. P. Magleby, and L. L. Howell: *A review of thickness-accommodation techniques in origami-inspired engineering*. Applied Mechanics Reviews **70**(1), 2018. doi: 10.1115/1.4039314.

[6] D. Melancon, B. Gorissen, C. J. Garca-Mora, C. Hoberman, and K. Bertoldi: *Multistable inflatable origami structures at the metre scale*. Nature **592**(7855), 545–550, 2021. doi: 10.1038/s41586-021-03407-4.

[7] I. Mustafa and T. H. Kwok: *Interlacing Infills for Multi-Material Fused Filament Fabrication Using Layered Depth Material Images*. Micromachines **13**(5), 773, 2022. doi: 10.3390/mi13050773.

[8] Y. Noma, K. Narumi, F. Okuya, and Y. Kawahara: *Pop-up print: Rapidly 3D printing mechanically reversible objects in the folded state*. In *Proceedings of the 33rd Annual ACM Symposium on User Interface Software and Technology*, 58–70. 2020.

[9] T. Tachi: *Geometric considerations for the design of rigid origami structures*. In *Proceedings of the International Association for Shell and Spatial Structures (IASS) Symposium*, vol. 12, 458–460. Elsevier Ltd Shanghai, China, 2010.

[10] T. Tachi: *Rigid-foldable thick origami*. Origami **5**(5), 253–264, 2011.

[11] J. Yin, C. Lu, J. Fu, Y. Huang, and Y. Zheng: *Interfacial bonding during multi-material fused deposition modeling (FDM) process due to inter-molecular diffusion.* Materials & Design **150**, 104–112, 2018. doi: 10.1016/j.matdes.2018.04.029.

[12] L. Zimmermann and T. Stanković: *Rigid and flat foldability of a degree-four vertex in origami.* Journal of Mechanisms and Robotics **12**(1), 011004, 2020. doi: 10.1115/1.4044737.

Received February 19, 2024; final form June 21, 2024.